Anharmonic phonon effects in Raman spectra of unsupported vertical graphene sheets

Jingjing Lin,[1] Liwei Guo,[1] Qingsong Huang,[1] Yuping Jia,[2] Kang Li,[1] Xiaofang Lai,[1] and Xiaolong Chen[1,*]

[1]*Research and Development Center for Functional Crystals, Beijing National Laboratory for Condensed Matter Physics, Institute of Physics, Chinese Academy of Sciences, P.O. Box 603, Beijing 100190, China*

[2]*Center for Condensed Matter and Material Physics, Beihang University, Beijing 100191, China*

(Received 25 September 2010; published 30 March 2011)

Temperature-dependent Raman scattering is performed on unsupported vertical graphene sheets, which are approximate to free graphene without supporting the substrate. Here the observed G peak line shift with temperature is completely consistent with the theoretical prediction based on the first-principles calculation on free graphene, and our result is helpful to understand intrinsic anharmonic phonon characteristics of free graphene and the divergence on the G peak line shift with temperature. However, the observed linewidth variation is different from the prediction. To reveal the origins, a simplified Klemens model is used, and the dominating anharmonic phonon scattering mechanism is explored. In addition, line shift and linewidth variations of D and 2D peaks of the graphene sheets with temperature are revealed, and the possible mechanisms dominating the results are discussed.

DOI: 10.1103/PhysRevB.83.125430 PACS number(s): 81.05.ue, 78.30.−j, 63.22.Rc, 81.10.St

I. INTRODUCTION

Graphene, a monolayer graphite sheet, exhibits many exotic and fantastic properties owing to its unique linear energy dispersion relation near the K point in its Brillouin zone.[1] Particularly, its exceptionally unique electronic properties, such as the half-integer quantum Hall effect at room temperature,[2] quantum transport of massless Dirac fermions,[3] extremely high mobility of its charge carriers,[4] and the potential for realizing ballistic conduction,[5] make graphene a promising candidate for ultrahigh-speed nanoelectronics.[6] Currently, many techniques have been used to identify this amazing material, such as optical microscopes,[7] x-ray photoelectron spectra,[8] low-energy electron diffraction,[9] scanning tunneling microscopes,[10] and Raman scattering,[11–13] etc. Among them, Raman scattering is considered a nondestructive technique for quick inspection of layer numbers[11,12] and the structural and electronic properties of graphene.[13] Particularly, temperature-dependent Raman scattering is important for further understanding some of the physical effects induced by anharmonic phonons, such as thermal expansion, specific heat, and thermal conductivity.[14–17] The anharmonic phonon effect is a combined effect of phonon-phonon (ph-ph) and electron-phonon (e-ph) interactions, which plays a key role in thermal expansion and carrier transport properties of materials. In addition, the anharmonic phonon properties of graphene are also a significant aspect for the design of efficient nanoelectronic devices.[15] Recently, the temperature-dependent Raman line shift of the G phonon mode have attracted significant attention[16–21] because it can be used to monitor laser-induced local temperature changes in graphene and carbon nanotubes to extract information on the thermal transport properties of these systems.[22–27] The superior thermal conductivity of graphene was deduced on the basis of the temperature coefficient of the Raman G peak shift with temperature, as reported in Ref. 16,17,22. However, it should be noted that the reported temperature coefficient of the G mode of graphene is diverse, ranging from -0.016 to -0.038 cm^{-1}/K depending on the fabrication method for graphene and the supporting substrate under the graphene layers.[16–21] Although the reported temperature effect on Raman spectra is not a substrate-induced property, it is difficult to rule out the contribution of the substrate to the single- or double-atomic-layer graphene from the measured data. Thus, exploring intrinsic anharmonic phonon characteristics of free graphene without a supporting substrate is necessary and imperative.

Here the temperature-dependent Raman scattering experiments were performed on unsupported vertical graphene sheets, where there is no surface contact among the graphene sheets and no contact with other matter except with the atmosphere where they are exposed. They are better approximate to a free graphene compared to the graphene layers reported by Refs. 16–21. Hence, by using these special graphene sheets, the substrate effects can be eliminated, and the intrinsic characteristics of graphene will be revealed to a more approximate extent. Moreover, according to the model calculation[28–30] of the temperature dependence of the line shift and linewidth combined with experimental data, it is inferred that the four-phonon process is dominant over the three-phonon process in the Raman line shift, while thermal expansion contributes a weak compensation effect to the Raman line shift. However, for the linewidth variation, it is found that the ph-ph interaction is the dominant factor in broadening G mode linewidth, while e-ph interaction narrows the linewidth slightly. Also, two other Raman modes of D and its overtone 2D have been studied, and their variation with temperature has been revealed systematically. To the best of our knowledge, there are few detailed reports on the D and 2D modes varying with temperature until now because the analysis of the D mode is considered to be difficult since the signal is strongly influenced by the defect density.[31] A different variation behavior in the linewidth of the two-phonon 2D mode from that of the one-phonon D mode is observed. The possible physical mechanisms behind the phenomena are discussed.

II. EXPERIMENTS

The unsupported vertical graphene sheets were grown on SiC substrates by using physical vapor transport (PVT) equipment. A commercially available 2-inch 4H-SiC (0001)

on-axis wafer (TankeBlue, Beijing) was used as a substrate for growing unsupported vertical graphene sheets. Before loading the SiC wafer in the PVT system, it was degreased with acetone and methanol, rinsed with deionized water, and blown dry with nitrogen gas. Then the SiC substrate was put into a graphite crucible and loaded into the PVT system. The SiC substrate was heated to 1600 °C in an atmosphere of argon and hydrogen mixing gas (95 vol % Ar + 5 vol % H_2), while decreasing the pressure in the PVT system from 50 kPa to 0.001 Pa in 5 min and then adding the mixing gas to the PVT system until the pressure reached 50 kPa and maintaining these conditions for 25 min. After repeating the pumping and filling procedure three times, the heat was turned off, and the temperature was cooled to room temperature naturally. A black film formed on the surface of the SiC substrate and was composed of densely arranged vertical graphene sheets with a height of 10–20 μm, as analyzed by scanning electron microscopy (SEM), which is shown in Fig. 1. To exclude the effect of the SiC substrate on Raman spectra of the measured vertical graphene sheets, the graphene sheets were peeled from the SiC substrate by annealing the SiC, on which the vertical graphene sheets were grown, at 500 °C for 6 h in air. After annealing, the ~20-μm-thick black film was separated from the SiC substrate and split into several pieces that were about a few centimeters in size. Three of them were used in our Raman scattering measurements.

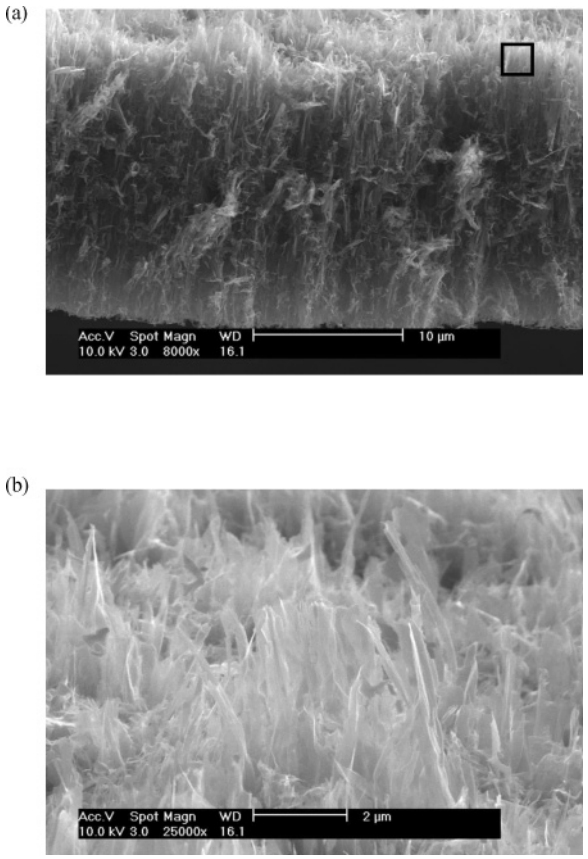

FIG. 1. The morphology of unsupported vertical graphene sheets: (a) SEM cross-section image and (b) magnified image of the local area in Fig. 1(a) indicated by the black square.

Raman scattering experiments were performed in a temperature range from 79 to 773 K, and the Raman signal was collected by a high-resolution Raman spectrometer HR800 with a 532-nm laser excitation focused to a spot about 1 μm in diameter with a power of 1 mW measured on top of the cold-hot cell window (correspondingly, it was much smaller on the sample surface) to avoid the effects of local heating on the sample. Our sample was placed on a 0.17-mm-thick quartz cover slip, and the cover slip, along with our sample, was put into the cold-hot cell of a commercial THMS600, which is a widely used stage for variable-temperature experiments and whose temperature is controlled by a TMS94 temperature controller in the temperature range from 77 to 873 K with an accuracy within ±0.1 K. The Raman scattering signal is recorded after the sample's temperature reaches the setting point and remains at that temperature for 3 min to make sure the temperature is steadily kept at the setting temperature. In addition, to avoid possible error induced by inhomogeneity in a sample, our Raman scattering measurement was performed on a fixed position on the sample while the temperature changed from high to low or vice versa. Three serial measurements were performed on three samples that were taken from the same 2-in. SiC wafer whose surface was covered with the unsupported vertical graphene sheets. During the Raman scattering measurement, the quartz cover slip merely acted as a support, and its contact with the bottom ends of the vertical graphene sheets was loose. Since the Raman excitation laser came from the top ends of the vertical graphene sheets whose heights were about 10–20 μm, the effect of the cover slip on the Raman scattering signal of the vertical graphene sheets can be neglected completely.

III. RESULTS AND DISCUSSION

Figure 1 shows the cross-section morphology of the graphene sheets analyzed by SEM, which is a typical morphology of the unsupported vertical graphene sheets we grew on the SiC substrate. Figure 1(a) shows that the graphene sheets are vertically standing like a naturally growing herbaceous plant and their heights are about 10–20 μm. In Fig. 1(b) the magnified image of the top area marked by the square in Fig. 1(a) shows that the graphene sheets are transparent, indicating it is a few-monolayer graphene, similar to the 1- to 4-monolayer graphene observed by transmission electron microscopy (TEM) in our previous work.[32] Meanwhile, it is noted that the graphene sheets show a similar feature of narrowing its width with its height. The shape is a benefit to enhanced field emission properties, as confirmed in our earlier work.[32] In addition, this kind of graphene is an ideal configuration for studying the intrinsic properties of graphene since a graphene structure that is a single atomic layer thick is easily interacts with other contact matters, especially its supporting substrate. Therefore, variable-temperature Raman scattering experiments were performed on the graphene sheets to explore its intrinsic anharmonic phonon effects and the physical mechanism behind the observed phenomena.

Figure 2 shows Raman scattering spectra of the unsupported vertical graphene sheets measured in a temperature range from 79 to 773 K. In Fig. 2, three typical Raman peaks are clearly observed. The prominent peak is a G peak positioned at

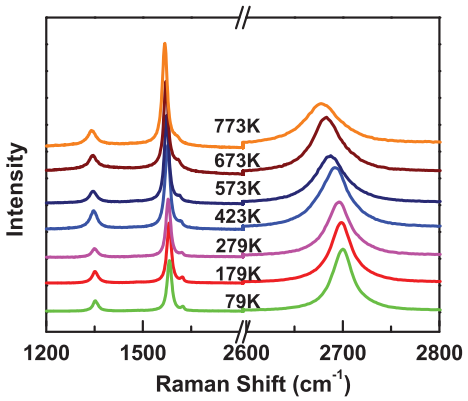

FIG. 2. (Color online) The typical Raman scattering spectra of the unsupported vertical graphene sheets measured in a temperature range from 79 to 773 K.

1580 cm^{-1}, with a linewidth of 16 cm^{-1} at room temperature, which is contributed by the degenerate phonon mode E_{2g} at the center of the Brillouin zone and is a typical representative of sp^2 carbon hybridization.[33] The D peak originates from a defect-assisted one-phonon process near the K point of the Brillouin zone which is sensitive to the domain size of graphene or the crystalline defects in graphene; its position is at 1350 cm^{-1}, with a linewidth of 22 cm^{-1} at room temperature. The 2D peak, an overtone of the D peak, which originates from a second-order phonon process involving two optical phonons near the K point, is located at about 2697 cm^{-1}, with a linewidth of 27 cm^{-1}at room temperature. It is noted that the 2D peaks measured at different temperatures are symmetric and can be well fitted by a single Lorentzian line shape. As is well known, the 2D peak is sensitive to the layer number of graphene and is often used to identify the layer number of graphene.[11,12] However, as seen in Fig. 1, the graphene sheets are not uniform in layer number, and the collected Raman signal is contributed by the vertical graphene sheet bunching at an area of the laser spot that has a diameter of about 1 μm. This fact suggests that different carbon honeycomb layers in the same graphene sheet are weakly coupled and behave like a single monolayer graphene in their Raman spectra.[34] In addition, the 27-cm^{-1} linewidth in the 2D peak is close to the best reported result (24 cm^{-1}) of a 2D peak from a monolayer graphene,[35] which means that the crystalline quality of our unsupported vertical graphene is as good as the ones prepared by other methods.[36] Furthermore, the narrow 2D peak linewidth indicates the graphene sheets covered by the laser spot have similar crystalline quality and stacking way of the adjacent layers in the same graphene sheet. In our situation, each of the graphene sheets is free standing vertically, and there is no surface contact among them. Therefore, the Raman features of the unsupported vertical graphene sheet bunching are approximate to a free graphene without any contact with other matter. A detailed analysis of the experimental data obtained here is helpful for revealing and understanding the intrinsic anharmonic properties of free graphene.

The temperature dependence of the G peak line shift and linewidth of the three samples measured in the temperature range from 79 to 773 K are shown in Fig. 3, where different symbols represent the measured data from different samples.

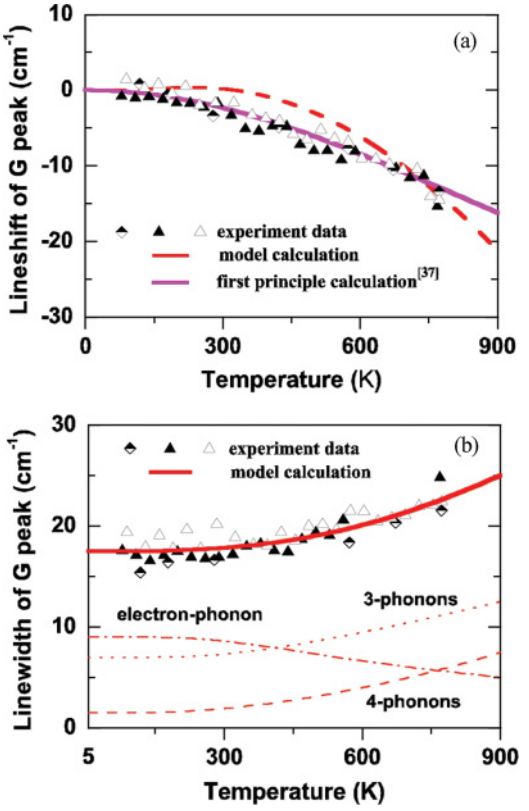

FIG. 3. (Color online) The temperature dependence of (a) the line shift and (b) the linewidth of the G peak measured in the temperature range from 79 to 773 K. The half-filled diamonds, filled triangles, and open triangles represent the experimental data of the three samples. In Fig. 3(a), the solid line is a theoretical prediction from Ref. 37, and the dashed line is a calculated result using the simple model. In Fig. 3(b), the solid line is a calculated result using the model including the contributions of three-phonon, four-phonon, and e-ph interactions, which are shown as a dotted line, dashed line, and dot-dashed line, respectively.

Here all of the experimental data about the G peak line shift as well as its linewidth are extracted from the Raman spectra, measured at different temperatures, fitted by a single Lorentzian function, where the relative zero point of the G mode line shift is taken as 1582 cm^{-1}, which is a G mode frequency at the low temperature of our samples. From Fig. 3(a), it is found that these experimental data from different samples are all matched well with a single curve. The result suggests that the characteristic of anharmonic phonons revealed by using unsupported vertical graphene sheets is not sample dependent, but an intrinsic behavior of a free graphene. Furthermore, the line shift variations with temperature are quite consistent with the theoretical prediction based on the first-principles calculation reported by Bonini *et al.*[37], as shown by the solid line in Fig. 3(a). Remarkably, the matching between our experimental data and theory for the G mode line shift with temperature indicates unsupported vertical graphene sheets are a good substitution for free graphene. According to the theoretical calculations,[37] it is known that a four-phonon process is dominant over both thermal expansion and three-phonon effects on G mode line shift with temperature. In Fig. 3(a), it is shown that the relationship of the G peak position

and temperature is nonlinear in the whole temperature range we measured. In the low-temperature range below 400 K, the G peak position changes slightly with temperature. However, in the high-temperature range above 400 K, the G peak line shift shows a clear linear tendency with temperature. To compare our results with other reported results,[17] a linear fitting was performed in the two temperature ranges. The slopes are -0.020 and -0.022 cm^{-1}/K in the lower- and higher-temperature ranges, respectively. The deduced slope of -0.020 cm^{-1}/K at its absolute value is more than 25% higher than that of -0.016 and -0.015 cm^{-1}/K for the single-layer and bilayer graphene reported by Calizo *et al.* for the temperature scale of 100–400 K.[17] We suppose the large difference can be ascribed to the supporting substrate under the single-layer or bilayer graphene. A further study of temperature-dependent Raman spectra of graphene lying on SiC substrates with different orientations is underway to explore the substrate functions on temperature-dependent Raman spectrum.

In addition to the origins of the G peak frequency shift, the G peak linewidth is another significant quality for uncovering the interactions of electrons and phonons, which is very important for designing and understanding graphene-based electronic devices. Figure 3(b) shows the temperature-dependent linewidth of the G mode in the whole temperature range from 79 to 773 K. The dependence of linewidth on temperature is also found to be nonlinear, and the linewidth is seen to broaden with increasing temperatures. However, it is noted that our experimental data on linewidth varying with temperature are completely different from the theoretical prediction by Bonini *et al.* based on the first-principles calculation,[37] although their calculation of the G mode line shift matches quite well with our experimental data. Bonini *et al.* predicted that the G peak linewidth would narrow with increasing temperature, while only considering contributions of the e-ph and three-phonon processes to G mode linewidth variation. However, our results are similar to the recent experimental observations by Berciaud *et al.*[31] on graphene monolayers, where G mode linewidth broadened with increasing temperature. In their study,[31] they supposed that the observed broadening might result from contributions from higher-order anharmonic phonon terms that become significant at high temperature.

In order to reveal the physical mechanism responsible for dominating the G mode temperature-dependent behavior, especially a G mode linewidth variation, a model is proposed to analyze our experimental results. In principle, the phonon frequency shift $\Delta\omega_{\mathbf{q}j}$ and linewidth $\Gamma_{\mathbf{q}j}$ can be deduced from $\Delta\omega_{\mathbf{q}j} = \mathrm{Re}[\Pi_{\mathbf{q}j}]$ and $\Gamma_{\mathbf{q}j} = -\mathrm{Im}[\Pi_{\mathbf{q}j}]$, with Re and Im being the real and imaginary parts and $\Pi_{\mathbf{q}j}$ being the anharmonic phonon contribution to the phonon self-energy, assuming that the absolute value of $\Pi_{\mathbf{q}j}$ is far less than the phonon frequency $\omega_{\mathbf{q}j}$ [38]. To simplify the calculation, at a certain temperature, the G mode frequency of graphene can be expressed as[28–30]

$$\omega(T) = \omega_0 + \Delta\omega, \quad \Delta\omega = \left[\frac{d\omega}{dT}\right]_V \Delta T + \left[\frac{d\omega}{dV}\right]_T \Delta V, \quad (1)$$

where ω_0 is the G mode frequency while T approaches 0 K; here we use $\omega_0 = 1582$ cm^{-1} to fit our experiment data. $\Delta\omega$ is the phonon frequency shift at temperature T, $\left[\frac{d\omega}{dT}\right]_V \Delta T$ is a frequency shift due to the self-energy variation induced by direct coupling of the phonon modes (sometimes referred to as the pure temperature effect), and $\left[\frac{d\omega}{dV}\right]_T \Delta V$ is a frequency shift due to the contribution from the thermal expansion in volume.

For the pure temperature effect, a simple Klemens model[28–30] is used, considering three-phonon and four-phonon interactions, to calculate the phonon contribution to the frequency shift.

$$\left[\frac{d\omega}{dT}\right]_V \Delta T = A\left[1 + \frac{2}{e^x - 1}\right] + B\left[1 + \frac{3}{e^y - 1} + \frac{3}{(e^y - 1)^2}\right], \quad (2)$$

$$x = \frac{\hbar\omega}{2kT}, \quad y = \frac{\hbar\omega}{3kT}$$

where coefficients A and B are constants, representing the contributions of three-phonon and four-phonon processes to the frequency shift, respectively. In addition to the pure temperature effect, the contribution from the thermal expansion effect to the Raman frequency shift can be deduced using the description of the Grüneisen constant model:[14]

$$\left[\frac{d\omega}{dV}\right]_T \Delta V = \omega_0 \exp\left(-3\gamma_G \int_0^T \alpha_a \, dT\right) - \omega_0, \quad (3)$$

where γ_G is the Grüneisen parameter of the graphene G mode, α_a is the thermal expansion coefficient of graphene, and T is the absolute temperature. We take $\gamma_G = 1.99$ (Ref. 39) and α_a from that of graphite[40] for the E_{2g} mode of graphene. To check the effectiveness of the model, the G mode line shift with temperature is shown as a red dashed line in Fig. 3(a), taking the adjustable parameters of A and B as -1 and -6 cm^{-1}, respectively. It is noted that the dashed line reasonably described the experimental data, indicating the simple model is good enough to study the anharmonic phonon effects semiquantitatively. The values of A and B are of the same order, which means both three-phonon and four-phonon processes contribute to the G mode line shift. However the absolute value of B is nearly 6 times that of A, indicating a four-phonon process is dominant over a three-phonon process in contributing to the G mode Raman frequency shift in the unsupported vertical graphene. This conclusion is completely consistent with the theoretical calculation given by Bonini *et al.*[37]

To explore the physical mechanism behind the linewidth broadening with increasing temperature, the model calculation is also adopted as discussed for G mode frequency shift with temperature. The temperature-dependent linewidth is contributed from two main parts, one being the ph-ph [$\Gamma^{\text{ph-ph}}(T)$] effect involving a phonon decaying into lower-energy phonons and the other being the e-ph effect [$\Gamma^{\text{e-ph}}(T)$], which involves a phonon creating an electron-hole pair. Thus, the linewidth $\Gamma(T)$ can be expressed as

$$\Gamma(T) = \Gamma^{\text{ph-ph}}(T) + \Gamma^{\text{e-ph}}(T), \quad (4)$$

where $\Gamma(T)$ is a linewidth of the G mode at temperature T.

For ph-ph scattering-induced broadening $\Gamma^{\text{ph-ph}}(T)$, the simple Klemens model[28–30] is adopted, as used by Balkanski *et al.*,[29] where both of the three-phonon and four-phonon processes are considered; thus,

$$\Gamma^{\text{ph-ph}}(T) = C\left[1 + \frac{2}{e^{\hbar\omega_0/2kT} - 1}\right] + D\left[1 + \frac{3}{e^{\hbar\omega_0/3kT} - 1} + \frac{3}{(e^{\hbar\omega_0/3kT} - 1)^2}\right], \quad (5)$$

where C and D are constants. In the high-temperature limit, the factors multiplied by C and D vary as T and T^2, respectively, where the first and the second terms in brackets represent the contributions of three-phonon and four-phonon processes to the linewidth, respectively.

The e-ph scattering-induced broadening $\Gamma^{\text{e-ph}}(T)$ is described by Fermi's golden rule:[37,41]

$$\Gamma_{\mathbf{q}}^{\text{e-ph}}(T) = \frac{4\pi}{N_{\text{k}}} \sum_{\mathbf{k},i,j} |g_{(\mathbf{k}+\mathbf{q})j,\mathbf{k}i}|^2 [f_{\mathbf{k}i}(T) - f_{(\mathbf{k}+\mathbf{q})f}(T)]\delta \times [\varepsilon_{\mathbf{k}i} - \varepsilon_{(\mathbf{k}+\mathbf{q})j} + \hbar\omega_{\mathbf{q}}], \quad (6)$$

where $\omega_{\mathbf{q}}$ is the phonon frequency in wave vector $\mathbf{q}$, the sum is on N_{k} $\mathbf{k}$ vectors, $f_{\mathbf{k}i}(T)$ is the Fermi-Dirac occupation at temperature T for an electron with energy $\varepsilon_{\mathbf{k}i}$, and δ is the Dirac delta.[37]

Similar to the simplified model used in the (Ref. 37), a simplified model for the temperature dependence of $\Gamma^{\text{e-ph}}$ for the G mode was used at a finite temperature T:[37,42]

$$\Gamma_{\mathbf{q}}^{\text{e-ph}}(T) = \Gamma_{\mathbf{q}}^{\text{e-ph}}(0)\left(\frac{1}{e^{-\hbar\omega_0/2kT} + 1} - \frac{1}{e^{\hbar\omega_0/2kT} + 1}\right), \quad (7)$$

where a linear-band dispersion around the Fermi energy is assumed, which is critically satisfied for graphene. Thus, linewidth variation with temperature is described as

$$\Gamma(T) = \Gamma^{\text{ph-ph}}(T) + \Gamma^{\text{e-ph}}(T) = C\left[1 + \frac{2}{e^{\hbar\omega_0/2kT} - 1}\right] + D\left[1 + \frac{3}{e^{\hbar\omega_0/3kT} - 1} + \frac{3}{(e^{\hbar\omega_0/3kT} - 1)^2}\right] + \Gamma_{\mathbf{q}}^{\text{e-ph}}(0)\left[\frac{1}{e^{-\hbar\omega_0/2kT} + 1} - \frac{1}{e^{\hbar\omega_0/2kT} + 1}\right] \quad (8)$$

where $\Gamma_{\mathbf{q}}^{\text{e-ph}}(0)$ is a linewidth of G mode at low temperature and its valve is 11.01 cm^{-1}, as reported.[41] Here $\Gamma_{\mathbf{q}}^{\text{e-ph}}(0) = 9\ \text{cm}^{-1}$ and G mode phonon energy $\hbar\omega_0 = 196.2$ meV are used in combination with C and D values of 7 cm^{-1} and 1.5 cm^{-1}, respectively, to get a very good fit to our experimental data of the G mode linewidth varying vs T, as shown in Fig. 3(b). From the model calculations, it is found that both the three-phonon and four-phonon processes contribute to the broadening of the G mode and that the three-phonon process is dominant over the four-phonon process in broadening the linewidth. Conversely, the e-ph process narrows the linewidth with increasing temperature. In Fig. 3(b), the contributions to the G mode linewidth from the three- and four-phonon processes and the e-ph process are given as dotted, dashed, and dot-dashed lines, respectively. Based on our model calculations, it is revealed that the four-phonon process should be included when analyzing G mode linewidth varying with temperature, and the scattering contributions from three and four phonons together with the e-ph interaction can well describe the variation of G mode linewidth with temperature.

Finally, we address the temperature dependence of the defect-related D mode and its overtone 2D mode of the unsupported vertical graphene sheets. The 2D mode is Raman active and the D mode is Raman forbidden in a perfective graphene. To the best of our knowledge, there are few detailed reports on the D and 2D modes varying with temperature up to now. Here the line shift and linewidth of the D and 2D modes varying with temperature are shown in Fig. 4.

Figure 4(a) shows that the D peak position shifts to low frequency with increasing temperature and that the shift trend is nonlinear. Considering that the D mode is a breathing mode of sp^2 atoms in rings,[43] the contribution from the thermal expansion effect to line shift is trivial. Therefore, the anharmonic phonon contributions from three-phonon and four-phonon processes should be considered for the one-phonon D mode, although the disorder-induced D mode is due to second-order Raman scattering involving a wave vector K phonon and another scattering event induced by a symmetry-breaking quasielastic scattering process such as a defect.[44] Similar to the model calculation of G mode line shift, the constants representing three-phonon and four-phonon contributions to the line shift are taken to be -1 and -2.5 cm^{-1}, respectively, to fit our experiment data well, while taking $\omega_0 = 1353$ cm^{-1}. In Fig. 4(a), the calculated curve expressed as a solid line fits our experimental data quite well. For the 2D mode of a two-phonon Raman scattering, which is also an overtone of the D mode, the temperature-dependent line shift shown in Fig. 4(c) is similar to that of the D mode. Therefore, the simplified model for one-phonon mode line shift was applicable to it, and the constants representing three-phonon and four-phonon contributions were taken as -5 and -23 cm^{-1}, respectively, while taking $\omega_0 = 2699$ cm^{-1}. It is seen that the contributions from the two anharmonic phonon processes to line shift variation fit our experiment data quite well, as shown in Fig. 4(c). In Figs. 4(a) and 4(c), the three-phonon and four-phonon contributions are separately drawn as dotted and dashed lines in the entire temperature range from 79 to 773 K, respectively. It is noted that both of the three-phonon and four-phonon processes contribute to the line shift of D and 2D modes, but the four-phonon process is absolutely dominant over the three-phonon process, especially at high temperature.

Figures 4(b) and 4(d) show the dependence of the D peak and 2D peak linewidths on temperature. It is seen that the variations of the two linewidths with temperature are clearly different. A nonlinear curve is found for the D peak linewidth, similar to that of the G peak, while a nearly linear variation is found for the linewidth of the 2D peak. For the one-phonon mode, a simple Klemens model can be used to analyze the origin of the Raman linewidth variation, as discussed above for the G mode situation. Here the simple model is used to discuss the D mode linewidth variation. It is found the simplified model calculation fits our experimental data very well while

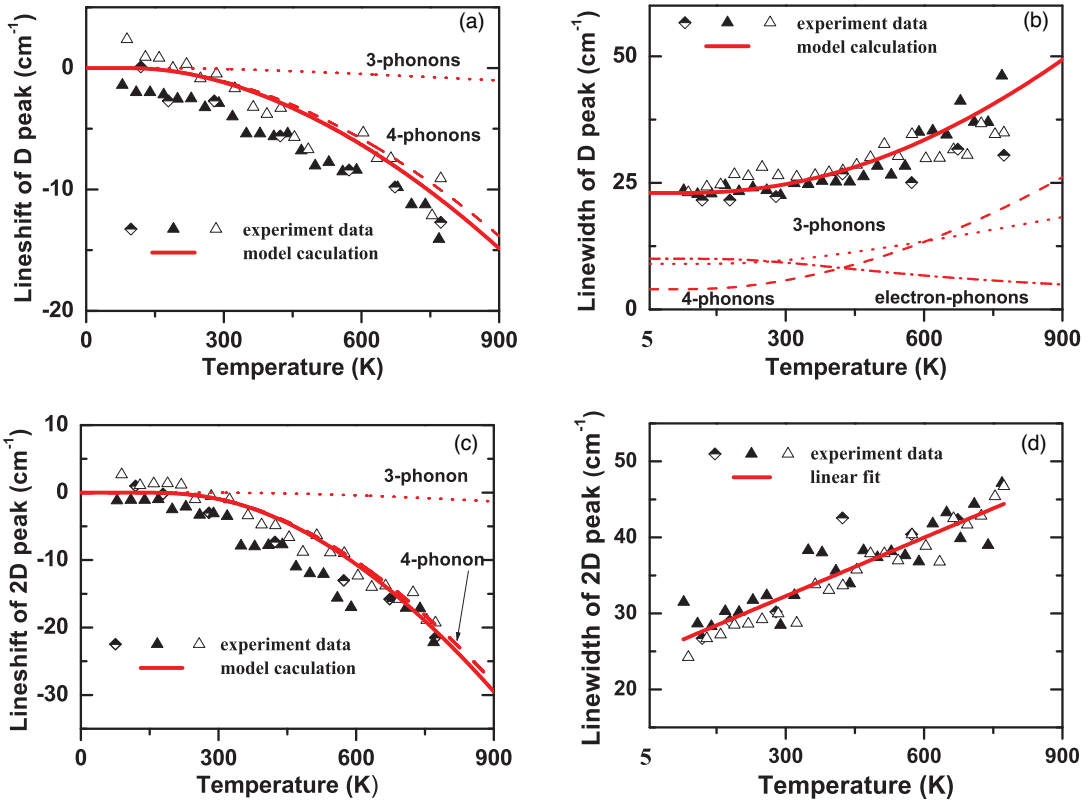

FIG. 4. (Color online) Temperature dependence of the line shift and linewidth of D and 2D peaks in the temperature range from 79 to 773 K. D peak (a) line shift and (b) linewidth and 2D peak (c) line shift and (d) linewidth vary with temperature; the half-filled diamonds, filled triangles, and open triangles are experimental data from the three samples, and the solid line is a model calculation result. The dotted line, dashed line, and the dot-dashed line represent the contributions from three-phonon, four-phonon, and e-ph interactions, respectively.

taking the constants representing the three- and four-phonon contributions to the linewidth as 9 and 4 cm^{-1}, respectively, and the D peak linewidth at low temperature as $\Gamma^{\text{e-ph}}(0) = 10\ cm^{-1}$, where contributions from three- and four-phonon processes and e-ph interaction to the D peak linewidth are shown as dotted, dashed, and dot-dashed lines, respectively. The result reveal that both three- and four-phonon scattering processes together with e-ph interaction take part in D peak linewidth broadening. For the linewidth of the 2D mode, a linear variation trend with a slope $-0.031\ cm^{-1}/K$ is found over the whole temperature range. In this case, the simplified model does not work well on the experimental data because the simplified model was developed for a one-phonon mode Raman scattering process. However, because the 2D mode is an overtone of the D mode and a two-phonon process with opposite momentum of the two phonons, the phonons with large momentum should be considered in the scattering process. Therefore, adapting the present simple model to suit a two-phonon Raman mode is necessary. The discussions above tell us that for the one-phonon mode, both the line shift and linewidth varying with temperature can be described well by the simplified model used here. However, for a two-phonon mode, such as the 2D mode, linewidth variation is a little different at low temperature, where e-ph scattering may be important, and should be considered in detail. This supposition should be proven by the first-principles calculation.

IV. SUMMARY

Temperature-dependent Raman spectra are performed in the temperature range from 79 to 773 K to explore the anharmonic phonon effects inherent in unsupported vertical graphene sheets, which is helpful for understanding the intrinsic anharmonic phonon characteristics of free graphene. In addition to examining the behavior of the G mode, the behavior of the D and 2D modes with temperature variation is revealed systematically. Here the variation of G peak line shift with temperature is quite consistent with the theoretical calculation based on the first-principles calculation on a free graphene. However, the observed linewidth variation, broadening with increasing temperature, is opposite to the theoretical prediction. The origins of the observed phenomena and the dominating anharmonic phonon-scattering mechanism were revealed based on a simplified Klemens model. For the G mode, the four-phonon process is a dominant contribution to line shift variation, while the three-phonon process is a dominant contribution to linewidth broadening. However, for the defect-assisted D mode, both three- and four-phonon processes contributed to line shift and linewidth variations. However, for the 2D mode of an overtone of the D mode, the linewidth variation is a little different from the one-phonon G and D modes in the low-temperature range, and a further theoretical calculation based on the first-principles calculation is necessary.

ACKNOWLEDGMENTS

The work was supported partly by the Knowledge Innovation Project of the Chinese Academy of Sciences under Grants No. KJCX2-YW-W22 and No. YYYJ-0701, the Ministry of Science and Technology of China under Grants No. 2007BAE34B00, No. 2007CB936300, and No. 2011CB932700, and the National Natural Science Foundation of China under Grants No. 51072223, No. 50972162, and No. 50702073.

*Corresponding author: chenx29@aphy.iphy.ac.cn

[1] K. S. Novoselov, A. K. Geim, S. V. Morozov, D. Jiang, Y. Zhang, S. V. Dubonos, I. V. Grigorieva, and A. A. Firsov, Science **306**, 666 (2004).

[2] K. S. Novoselov, Z. Jiang, Y. Zhang, S. V. Morozov, H. L. Stormer, U. Zeitler, J. C. Maan, G. S. Boebinger, P. Kim, A. K. Geim, Science **315**, 1379 (2007).

[3] K. Nomura and A. H. MacDonald, Phys. Rev. Lett. **98**, 076602 (2007).

[4] K. I. Bolotin, K. J. Sikes, Z. Jiang, M. Klima, G. Fudenberg, J. Hone, P. Kim, and H. L. Stormer, Solid State Commun. **146**, 351 (2008).

[5] X. Du, I. Skachko, A. Barker, and E. Andrei, Nat. Nanotechnol. **3**, 491 (2008).

[6] A. K. Geim and K. S. Novoselov, Nat. Mater. **6**, 183 (2007).

[7] L. Gao, W. Ren, F. Li, and H. M. Cheng, ACS Nano **2**, 1625 (2008).

[8] J. Penuelas, A. Ouerghi, D. Lucot, C. David, J. Gierak, H. Estrade-Szwarckopf, and C. Andreazza-Vignolle, Phys. Rev. B **79**, 033408 (2009).

[9] D. A. Siegel, S. Y. Zhou, F. El Gabaly, A. K. Schmid, K. F. McCarty, and A. Lanzara, Phys. Rev. B **80**, 241407(R) (2009).

[10] E. Stolyarova, D. Stolyarov, L. Liu, K. T.Rim, Y. Zhang, M. Han, M. Hybersten, P. Kim, and G. Flynn, J. Phys. Chem. C **112**, 6681 (2008).

[11] D. S. Lee, C. Riedl, B. Krauss, K. Von Klitzing, U. Starke, and J. H. Smet, Nano Lett **8**, 4320 (2008).

[12] D. Graf, F. Molitor, K. Ensslin, C. Stampfer, A. Jungen, C. Hierold, and L. Wirtz, Nano Lett **7**, 238 (2007).

[13] M. S. Dresselhaus, A. Jorio, M. Hofmann, G. Dresselhaus, and R. Saito, Nano Lett **10**, 751 (2010).

[14] C. Postmus, J. Ferraro, and S. Mitra, Phys. Rev. **174**, 983 (1968).

[15] N. Bonini, R. Rao, A. M. Rao, N. Marzari, and J. Menéndez, Phys. Status Solidi B **245**, 2149 (2008).

[16] I. Calizo, F. Miao, W. Bao, C. N. Lau, and A. A. Balandin, Appl. Phys. Lett. **91**, 071913 (2007).

[17] I. Calizo, A. A. Balandin, W. Bao, F. Miao, and C. N. Lau, Nano Lett **7**, 2645 (2007).

[18] L. M. Malard, R. L. Moreira, D. C. Elias, F. Plentz, E. S. Alves, and M. A. Pimenta, J. Phys. Condens. Matter **22**, 334202 (2010).

[19] M. J. Allen, J. D. Fowler, V. C. Tung, Y. Yang, B. H. Weiller, and R. B. Kaner, Appl. Phys. Lett. **93**, 193119 (2008).

[20] L. Zhang, Z. Jia, L. Huang, S. O'Brien, and Z. Yu, J. Phys. Chem. C **112**, 13893 (2008).

[21] D. Abdula, T. Ozel, K. Kang, D. G. Cahill, and M. Shim, J. Phys. Chem. C **112**, 20131 (2008).

[22] A. A. Balandin, S. Ghosh, W. Bao, I. Calizo, D. Teweldebrhan, F. Miao, and C. N. Lau, Nano Lett. **8**, 902 (2008).

[23] S. Ghosh, I. Calizo, D. Teweldebrhan, E. P. Pokatilov, D. L. Nika, A. A. Balandin, W. Bao, F. Miao, and C. N. Lau, Appl. Phys. Lett. **92**, 151911 (2008).

[24] Y. H. Lee and J. H. Lee, Appl. Phys. Lett. **96**, 083101(2010).

[25] W. Cai, A. L. Moore, Y. Zhu, X. Li, S. Chen, L. Shi, and R. S. Ruoff, Nano Lett. **10**, 1645 (2010).

[26] C. Faugeras, B. Faugeras, M. Orlita, M. Potemski, R. Nair, and A. K. Geim, ACS Nano **4**, 1889 (2010).

[27] I. K. Hsu, R. Kumar, A. Bushmaker, S. B. Cronin, M. T. Pettes, L. Shi, T. Brintlinger, M. S. Fuhrer, and J. Cumings, Appl. Phys. Lett. **92**, 063119 (2008).

[28] P. G. Klemens, Phys. Rev. **148**, 845 (1966).

[29] M. Balkanski, R. F. Wallis, and E. Haro, Phys. Rev. B **28**, 1928 (1983).

[30] E. S. Zouboulis and M. Grimsditch, Phys. Rev. B **43**, 12490 (1991).

[31] S. Berciaud, M. Y. Han, K. F. Mak, L. E. Brus, P. Kim, and T. F. Heinz, Phys. Rev. Lett. **104**, 227401 (2010).

[32] Q. S. Huang, G. Wang, L. W. Guo, Y. P. Jia, J. J. Lin, K. Li, W. J. Wang, and X. L. Chen, Small **7**, 450 (2011).

[33] A. C. Ferrari, J. C. Meyer, V. Scardaci, C. Casiraghi, M. Lazzeri, F. Mauri, S. Piscanec, D. Jiang, K. S. Novoselov, S. Roth, and A. K. Geim, Phys. Rev. Lett. **97**, 187401 (2006).

[34] Q. S. Huang, L. W. Guo, W. J. Wang, G. Wang, W. Y. Wang, Y. P. Jia, J. J. Lin, K. Li, and X. L. Chen, Chin. Phys. Lett. **27**, 046803 (2010).

[35] L. M. Malard, M. A. Pimenta, G. Dresselhaus, and M. S. Dresselhaus, Phys. Rep. **473**, 51 (2009).

[36] A. Geim, Science **324**, 1530 (2009).

[37] N. Bonini, M. Lazzeri, N. Marzari, and F. Mauri, Phys. Rev. Lett. **99**, 176802 (2007).

[38] M. Lazzeri, M. Calandra, and F. Mauri, Phys. Rev. B **68**, 220509 (2003).

[39] T. M. G. Mohiuddin, A. Lombardo, R. R. Nair, A. Bonetti, G. Savini, R. Jalil, N. Bonini, D. M. Basko, C. Galiotis, N. Marzari, K. S. Novoselov, A. K. Geim and A. C. Ferrari, Phys. Rev. B **79**, 205433 (2009).

[40] D. K.L. Tsang, B. J. Marsden, S. L. Fok, and G. Hall, Carbon **43**, 2902 (2005).

[41] M. Lazzeri, S. Piscanec, F. Mauri, A. C. Ferrari, and J. Robertson, Phys. Rev. B **73**, 155426 (2006).

[42] S. Piscanec, M. Lazzeri, F. Mauri, A. C. Ferrari, and J. Robertson, Phys. Rev. Lett. **93**, 185503 (2004).

[43] A. C. Ferrari and J. Robertson, Phys. Rev. B **61**, 14095 (2000).

[44] A. Jorio, R. Satio, G. Dresselhaus, and M. S. Dresselhaus, *Raman Spectrascopy in Graphene Related Systems* (Wiley-VCH, Berlin, 2011), Chap. 4, pp. 88–89.